# FEASIBILITY OF AMORPHOUS BONDING IN THERMOPLASTIC COMPOSITES AND THE RESULTING INTERLAMINAR RESIDUAL STRESSES

Joseph G. Kirchhoff[1], Tyler B. Hudson[2], Mehran Tehrani[3]
1- Walker Department of Mechanical Engineering, University of Texas at Austin, Austin, TX
2- NASA Langley Research Center, Hampton, VA
3- Department of Structural Engineering, University of California San Diego, San Diego, CA

## ABSTRACT

During rapid processing of thermoplastic composites, such as automated fiber placement manufacturing, crystallization is suspected to limit full polymer healing on the interfaces. Reptation theory suggests that interdiffusion can persist until temperature falls below the glass transition temperature in amorphous polymers; however, studies indicate that a critical crystallization value hinders interdiffusion for semi-crystalline polymers. This motivates the incorporation of a thin (5-20 $\mu$m) polyetherimide layer between low-melting polyaryletherketone interfaces. This paper will share results of vacuum bag-only processing fabricated short beam strength samples with varied thermal histories. Specifically, this work investigates the feasibility of processing the amorphous interfaces below the melt temperature of the semi-crystalline layer to prevent crystal melting during processing. It also examines the theoretical development of residual stresses, based on classical laminate theory, arising from mismatches in the coefficient of thermal expansion between the two polymers. In conclusion, this paper presents a novel approach to thermoplastic composite processing that could facilitate high-rate manufacturing and also sheds light on mechanics of failure in such samples.

Keywords: thermoplastic composites, polymer healing, fusion bonding, solidification

Corresponding author: joseph.g.kirchhoff@nasa.gov

## 1. INTRODUCTION

The interest in the manufacturability of large-scale (e.g., fuselages, wing structures, etc.) thermoplastic composite (TPCs) aerostructures stems from their exceptional toughness, recyclability, and chemical resistance. Notably, TPCs can be welded to eliminate the need for conventional fasteners or adhesive bonding and offer manufacturing flexibility and repair. This has led to an emphasis on high-rate technologies (> 60 airplanes/month) like thermoplastic automated fiber placement (AFP), thermal welding, and filament winding. Central to these methods is fusion bonding, which involves intimate contact, interdiffusion, and solidification [1]. Intimate contact refers to the polymer-polymer contact necessary for interdiffusion, where polymer chains cross interfaces and entangle. Interdiffusion continues in amorphous polymers until the glass transition temperature ($T_g$) [2] but ceases in semi-crystalline polymers upon a critical crystallization [3]. Crystallization, while crucial for fiber-matrix adhesion and chemical resistance, limits interdiffusion in high-rate settings as shown by Boiko et al. [3]. This study aims to address

*SAMPE Conference Proceedings. Indianapolis, IN, May 19-22, 2025. Society for the Advancement of Material and Process Engineering – North America. Any mention of commercial products and companies are for accurate reporting only and not intended as NASA endorsements.*

(DOI will be added by SAMPE)

the reduced processing window due to the onset temperature of critical crystallization by adding an amorphous polymer at the bonding interface.

A concept of amorphous bonding was introduced with a dual-bonding process called Thermabond© where an amorphous polymer polyetherimide (PEI) film was added to the surface of Aromatic Polymer Composite (APC-2) composites during hot pressing before subsequent welding [4], [5]. More recently, hybrid composite tapes have been developed by sandwiching carbon fiber reinforced polyetheretherketone (CF/PEEK) (127 µm) between neat PEI (50 µm) to promote amorphous bonding in high-rate settings [6]. A key benefit of the PEI film is that interdiffusion can occur below the melt temperature of the PEEK such that existing crystallinity does not melt during processing. The limitation of these approaches is that the addition of PEI reduces the relative fiber volume fraction of the composite (see Figure 1) leading to an expected decrease in mechanical performance. Arquier et al. show that the short beam strength (SBS) decreases by ~40% as resin-rich interlayer thickness increases from 5 to 13 µm [7]. This study investigates the optimal thickness of PEI necessary for amorphous bonding with minimal compromise of the fiber volume fractions (measured via optical microscopy). This innovation is aptly named Out-of-autoclave Amorphous/semi-crystalline Thermoplastic Materials for Aerospace-grade Energy-efficient Laminates (OATMEAL) for having the not too little or too much amorphous polymer and being processed in the Goldilocks window (between the $T_g$ of the amorphous polymer and the $T_m$ of the semi-crystalline polymer). Semi-crystalline plates with variable thickness of amorphous polymer are healed together below the $T_m$ of the semi-crystalline polymer and then SBS tested. There is a knockdown in SBS with the addition of PEI potentially due to the theoretical residual stresses that arise from the mismatch in CTE of the two polymers. This is investigated using classical laminate theory.

## 2. EXPERIMENTATION

### 2.1 Fabrication of Composite Laminates with Interlayers

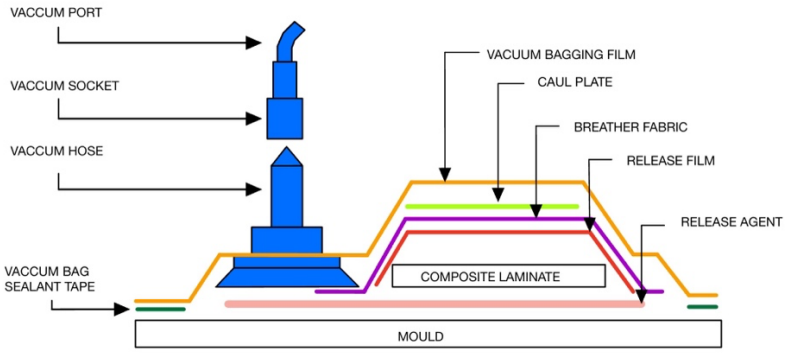


**Fig 1.** High-temperature vacuum bag setup used during experiments.

The semi-crystalline prepreg used in this study was unidirectional carbon fiber reinforced low melt polyaryletherketone (LM-PAEK™), with dimensions of 6.35 × 0.19 mm and a nominal fiber volume fraction of 55%, supplied by SUPREM. LM-PAEK has a melt temperature of 303°C. A two-step vacuum bagging process (shown in Figure 1) was employed to simulate the amorphous bonding concept with varying amounts of polyetherimide (PEI), commonly known as Ultem 1000,

which was supplied by Piezopvdf as a 5 micron-thick (nominal) neat polymer film. Materials for processing at thermoplastic temperatures (> 180°C) were sourced from Airtech, including Thermflex bagging film, Airweave UHT 800 breather, and Fast Tack HT sealant tape. The vacuum port and hose were Vac Valve 429 and Airflow 800, respectively. To prepare the steel mold, three layers of Frekote were applied to clean and seal surface cracks on the mold surface.

In the first step, two "half-plates" (96 × 160 mm) unidirectional $[0]_{14}$ LM-PAEK laminates were consolidated with PEI film on the tool-side surface using the vacuum bagging process in an oven at 360°C for 30 minutes. The half-plates were then cooled slowly inside the oven to room temperature to maximize crystallinity. The PEI films were applied in varying thicknesses (5, 10, 15, and 20 microns) by stacking multiple films in 40 mm sections. After consolidation, the half-plates were cut into six 32 × 160 mm sections along the 96 mm direction.

The second step involved the amorphous bonding of two half-plate sections to form a $[0_{14}/\mathrm{PEI}/0_{14}]$ laminate with PEI films at the midline. This bonding process was tested at 230°C, 280°C, and 360°C. After the bonding process, instead of slow oven cooling, the samples were air-cooled by removing them from the oven. This cooling method was selected to simulate higher cooling rates typically seen in high-rate processes (e.g., automated fiber placement, thermoforming). The glass transition temperature ($T_g$) of PEI is 216°C, so the PEI film is expected to heal at all the selected bonding temperatures, although the melt temperature ($T_m$) of LM-PAEK is 303°C.

### 2.2 Short Beam Strength Testing

Testing was conducted in accordance with the ASTM D2344 standard. Samples were cut to dimensions of 6 × 18 mm using a diamond wet saw. Due to noticeable thickness variations between samples, two different span lengths were used during testing to adhere to the standard requirements. However, testing protocols were adjusted to account for the resin-rich PEI interlayer. Instead of stopping the test after a 30% drop in load, as specified in the standard, testing was terminated after a 10% drop in load. This adjustment was made because, in specimens with less bonding, the LM-PAEK half-plates were able to continue carrying load even after the PEI interlayer had failed. The failure mechanism was categorized based on visual observations, with failure typically occurring in the PEI interlayer, resulting in the separation of the two half-plates.

### 2.3 Cross Sectional Microscopy

Cross-sectional inspection of both the fabricated samples and feedstock was performed using optical microscopy. Sections of interest, identified via C-Scan, were cut from the samples using a diamond saw, potted in epoxy, and then sanded progressively from 80 grit to 2000 grit using a Struers polishing machine. Final polishing was completed with a 1 μm suspension fluid. Imaging of the polished sections was conducted using a Reichert MEF4M microscope.

## 3. RESIDUAL STRESS PREDICTIONS

Classical laminate theory (CLT) is used to predict the residual stress arising from manufacturing. The primary goal is to capture the variation in CTE through the thickness, resulting from the use of two different polymer systems and resin-rich interlayers. For this analysis, carbon fiber

reinforced PEEK (AS4/APC-2) instead of CF/LM-PAEK, is used, as the material properties are better characterized in the literature [8]. The resin-rich PEI interlayers are treated as individual laminae. PEKK is also a more suitable candidate for OATMEAL due to the $T_m$ of PEEK being ~40 ℃ higher than that of LM-PAEK, creating a wider Goldilocks window. To predict the residual stresses during cooling from 300°C to 25°C ($\Delta T = 275$) using CLT, the material properties of the laminate (Young's modulus, Poisson's ratio, CTE, etc.) and the stacking sequence are defined. The assumptions made during this analysis include:

1. Linear elastic behavior of the materials.
2. A plane stress condition.
3. Perfect bonding between layers.
4. Material property homogeneity within a layer.
5. Constant material properties (independent of temperature).

Importantly, it is acknowledged that while the carbon fiber reinforced PEEK exhibits transversely isotropic properties due to its fiber alignment and resin characteristics, the resin-rich PEI interfaces are isotropic, demonstrating uniform properties in all directions. The material properties used are:

Transversely isotropic CF/PEEK (AS4/APC-2) [8]:

- **Elastic moduli:** $\mathrm{E}_1 = 135$ GPa, $\mathrm{E}_2 = 10.0$ GPa, $\mathrm{G}_{12} = 5.2$ GPa
- **Poisson's ratios:** $\nu_{12} = 0.35$
- **Coefficient of thermal expansion (CTE):** $\alpha_1 = 0.5 \times 10^{-6}/℃$, $\alpha_2 = 30.0 \times 10^{-6}/℃$

Isotropic PEI (Ultem 1000):

- **Elastic modulus:** $\mathrm{E} = 7.91$ GPa**,** $\mathrm{G} = 7.91$ GPa
- **Poisson's ratios:** $\nu = 0.37$
- **CTE:** $\alpha = 55.8 \times 10^{-6}/℃$

The analysis begins with calculating the stiffness matrix (inverse of the compliance matrix) for the individual lamina under the plane stress assumption, shown for the isotropic PEI and transversely isotropic CF/PEEK layers,

$$\mathrm{Q_{iso}} = \begin{bmatrix} \frac{\mathrm{E}}{1-\nu^2} & \frac{\nu \mathrm{E}}{1-\nu^2} & 0 \\ \frac{\nu \mathrm{E}}{1-\nu^2} & \frac{\mathrm{E}}{1-\nu^2} & 0 \\ 0 & 0 & \frac{\mathrm{G}}{2} \end{bmatrix} \qquad \mathrm{Q_{tiso}} = \begin{bmatrix} \frac{\mathrm{E_1}}{1-\nu_{12}\nu_{21}} & \frac{\nu_{12}\mathrm{E_2}}{1-\nu_{12}\nu_{21}} & 0 \\ \frac{\nu_{12}\mathrm{E_2}}{1-\nu_{12}\nu_{21}} & \frac{\mathrm{E_2}}{1-\nu_{12}\nu_{21}} & 0 \\ 0 & 0 & \frac{\mathrm{G_{12}}}{2} \end{bmatrix}.$$

This is the stiffness matrix in the principal material coordinate system ($\mathbf{Q}$). For a lamina with a fiber orientation angle (θ), the stiffness matrix is transformed to the global coordinate system ($\overline{\mathbf{Q}}$) using a transformation matrix, typically derived using the angle transformation of stiffness tensors,

$$\overline{\mathbf{Q}} = \mathbf{T^T Q T},$$

where the transformation matrix T for a 2D case is

$$\mathbf{T} = \begin{bmatrix} \cos^2\theta & \sin^2\theta & 2\sin\theta\cos\theta \\ \sin^2\theta & \cos^2\theta & -2\sin\theta\cos\theta \\ -\sin\theta\cos\theta & 2\sin\theta\cos\theta & \cos^2\theta - \sin^2\theta \end{bmatrix}.$$

The **ABD** matrix is a 6x6 matrix that relates the applied forces and moments to the mid plane strains in the laminated composite. The matrix is formed by integrating the stiffness matrices of the individual layers over the thickness of the laminate. The form of the **ABD** matrix,

$$\begin{bmatrix} \mathbf{A} & \mathbf{B} \\ \mathbf{B^T} & \mathbf{D} \end{bmatrix},$$

where:

- **A** is the extensional stiffness matrix (relates forces to in-plane strains),
  - $\mathbf{A} = \sum_{i=1}^{n} \bar{\mathbf{Q}}_i \, t_i$
- **B** is the coupling matrix (relates moments to in-plane strains),
  - $\mathbf{B} = \sum_{i=1}^{n} \bar{\mathbf{Q}}_i (z_i t_i)$
- **D** is the bending stiffness matrix (relates moments to curvatures).
  - $\mathbf{D} = \sum_{i=1}^{n} \bar{\mathbf{Q}}_i (z_i^2 t_i)$

In this study, the laminates of interest are all symmetric and balanced such that there is no **B** contribution. Specifically, the shown laminates for the analysis are:

- $[0/\mathrm{PEI}/0]$: to match the layup used in the experimental section.
- $[\mathrm{PEI}/0/\mathrm{PEI}]_{2s}$: to consider a unidirectional laminate with PEI bonding (OATMEAL).
- $[0/\mathrm{PEI}/90/\mathrm{PEI}/0]$: to consider an off-axis laminate with PEI bonding (OATMEAL).

The residual stresses arise from thermal shrinkage upon cooling. The thermal forces are first calculated in every layer as

$$\begin{Bmatrix} N_x^T \\ N_y^T \\ N_{xy}^T \end{Bmatrix} = \Delta T \sum_{i=1}^{n} \bar{\mathbf{Q}}_\mathbf{i} \begin{Bmatrix} \alpha_x \\ \alpha_y \\ \alpha_{xy} \end{Bmatrix}_i t_i \,,$$

where the CTE are transformed from the material coordinate system to the global coordinate system (the x, y nomenclature) via the transformation matrix,

$$\boldsymbol{\alpha}_{\mathbf{global}} = \mathbf{T}(\theta)\, \boldsymbol{\alpha}$$

The **ABD** matrix is now used to determine the mid-plane strains $\{\boldsymbol{\varepsilon}^{\mathbf{0}}\}$, but since the chosen laminates are symmetric and balanced this is simplified to

$$\begin{Bmatrix} N_x^T \\ N_y^T \\ N_{xy}^T \end{Bmatrix} = \mathbf{A} \begin{Bmatrix} \varepsilon_x^0 \\ \varepsilon_y^0 \\ \varepsilon_{xy}^0 \end{Bmatrix}$$

Now, using the mid-plane strain, the residual stress arising in each layer can be predicted through

$$\begin{Bmatrix} \sigma_x \\ \sigma_y \\ \sigma_{xy} \end{Bmatrix}_i = \bar{\mathbf{Q}}_\mathbf{i} \begin{Bmatrix} \varepsilon_x^0 - \Delta T \alpha_x \\ \varepsilon_y^0 - \Delta T \alpha_y \\ \varepsilon_{xy}^0 - \Delta T \alpha_{xy} \end{Bmatrix}_i$$

This analysis is done to investigate the residual stress that develops in the resin-rich, isotropic, PEI layers during manufacturing ($\Delta T = 275°C$). These stresses arise due to a mismatch in CTE between the resin-rich PEI and the CF/PEEK. This analysis is limited to in-plane stresses as a more advanced model is required for accurate prediction of interlaminar stresses (relevant to SBS) [9].

# 4. RESULTS

## 4.1 SBS Testing

The SBS results, shown in Figure 2, are informative of how well consolidated the thermoplastic panels are. Representative force-displacement curves were selected to highlight how premature failure of the PEI interlayer, common in 230°C and 280°C samples, can be misleading. In these cases, once the PEI interlayer fails prematurely, the LM-PAEK half plates continue to bear the load and undergo plastic deformation, leading to significant displacement before a final failure occurs. While ASTM D2344 recommends using a 30% load drop to define peak load, the authors opted for a 10% drop to better capture the initial failure of the PEI layer. For instance, in the 230°C 5 μm sample (Figure 2, left, blue curve), the SBS values are 105.40 MPa and 78.66 MPa for the 30% and 10% load drop-off criteria, respectively. The 30% drop more accurately reflects failure in the LM-PAEK half plates, while the 10% drop provides a more accurate representation of the PEI interlayer's healing phenomena. Figure 2 (right) demonstrates the samples that failed prematurely in the PEI interlayer as star markers. As the processing temperature increased, the failure mode shifted from premature PEI failure to more complex plastic failure and delamination in the LM-PAEK. At 280°C some of the samples failed prematurely, particularly the thicker PEI interlayers suggesting that adding too much polymer may reduce performance.

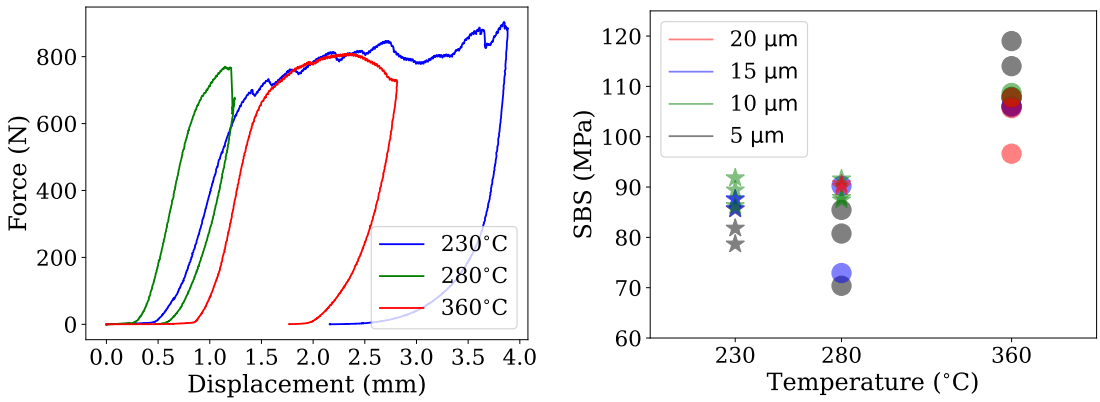


**Fig 2.** (Left) Representative loading curves from SBS with 5-micron, (Right) SBS data of specimens taken from the $[0]_{28}$ plate with stars showing premature failure in the PEI.

At lower temperatures, the 10 and 15 µm PEI interlayers outperform the 5 µm interlayer. However, at 360°C, the 5 µm interlayer exhibited superior performance. This result aligns with findings in Arquier et al. [7], where thicker interlayers led to a reduction in SBS. It seems that, with sufficient interdiffusion, interlayer thickness becomes a critical factor. At lower temperatures with incomplete healing, a thicker interlayer may help. It is important to note that, SBS is a complex phenomenon and does not correspond to a simple shear failure at the midplane, as visible plastic deformation during loading occurs in the samples. The time allowed for interdiffusion is crucial to improving SBS performance. Using AFP to fabricate CF/LM-PAEK laminates, SBS typically averages around 50 MPa [10], but the fast-cooled samples in Figure 2 show a significantly higher SBS. This study's experiment is limited due to the fact that only a single interlayer of PEI was added; It would be interesting to explore the SBS knockdown from adding PEI to consolidate every laminate. The knockdown in strength may be worth the manufacturing flexibility afforded by the amorphous bonding. A key advantage of the amorphous layer is that it is less sensitive to cooling rate when processed below the melt temperature of LM-PAEK, facilitating interdiffusion regardless of cooling conditions.

### 4.2 Optical Microscopy

Cross-sectional imaging of the laminates were used to measure the PEI interlayer thickness. Figure 3 shows example cross-sections to illustrate how increasing the PEI thickness on the half plate was consistent with the final part interlayer thickness. During processing of the half plates, the LM-PAEK was melted to allow for the glassy PEI to heal together and it is observed that there is some fiber repopulation into the PEI film. This effect is more exemplified in the full plates that processed at 360°C as the LM-PAEK was melted for a second time. In the 5 µm 360°C sample, an interlayer thickness greater than 10 µm was observed (see Figure 3a). This is potentially due to flow of LM-PAEK during processing. Whereas, in the case of 360°C, 20 $\mu$m-thick PEI sample, the interlayer thickness varied from ~20 µm to ~50 µm suggesting an uneven PEI distribution (see Figure 3b). The authors contribute this is potentially due to the difficulty of handling 5 µm films during layup of the half-plates or resin flow during manufacturing. In the case of the samples healed beneath the melt temperature of LM-PAEK (see Figure 3b,c) incomplete interdiffusion was observed. There are visible tiny cracks at the interfaces where intimate contact did not have sufficient time to complete which implies incomplete interdiffusion.

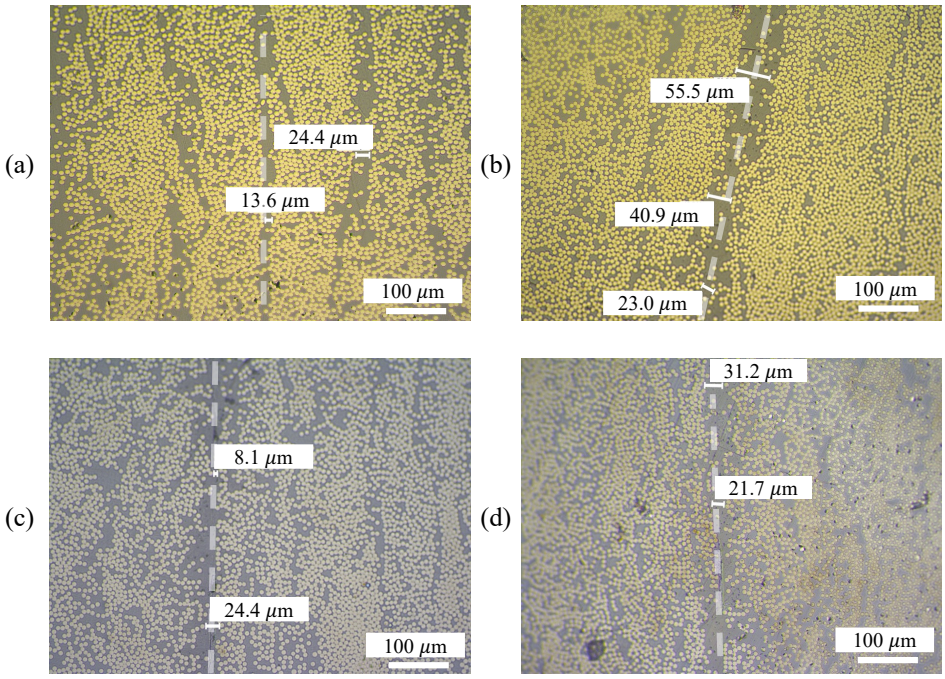


**Fig 3.** Optical cross-section imaging of (a) 380°C, 5 $\mu$m-thick PEI, (b) 360°C, 20 $\mu$m-thick PEI, (c) 230°C, 5 $\mu$m-thick PEI, and (d) 280°C, 10 $\mu$m-thick PEI.

### 4.3 Residual Stress Predictions

As shown in Figure 3, distinct resin-rich layers of PEI are present, which have higher CTE than the surrounding composite material in the axial direction. This different CTE leads to the development of residual stresses, as the variation in thermal strains restricts the free movement of the layers. These residual stresses persist into the service of the part acting as a preload reducing the laminates performance. Using CLT, the resin-rich PEI layers are modeled as isotropic lamina along with the transversely isotropic CF/PEEK lamina to predict the theoretical residual stresses arising during cooling. Although there is some fiber repopulation into the PEI layers, the residual stress analysis conducted assumes the layer is fully neat PEI. Additionally, the experimental section was conducted using CF/LM-PAEK as the semi-crystalline composite, but the analysis is done with CF/PEEK as the properties are more readily available. The in-plane (tensile and compressive) residual stresses is found for three laminates. Figure 4 is the predictions for a $[0/\mathrm{PEI}/0]$ laminate; this stacking sequence is akin to the experimental section of this study. The analysis predicts a tensile residual stress of 16.25 and 15.91 MPa in the PEI layer for 5 and 25 µm thickness, respectively. Since PEI ($\alpha = 55.8 \times 10^{-6}/°\mathrm{C}$) has a larger CTE than both the CF/PEEK CTEs ($\alpha_{12} = 0.5 \times 10^{-6}/°\mathrm{C}$, $\alpha_{21} = 30.0 \times 10^{-6}/°\mathrm{C}$), the resin-rich layer cannot fully shrink and is hence held in tension by the CF/PEEK layers. The CF/PEEK layers are compressed to maintain force balance.

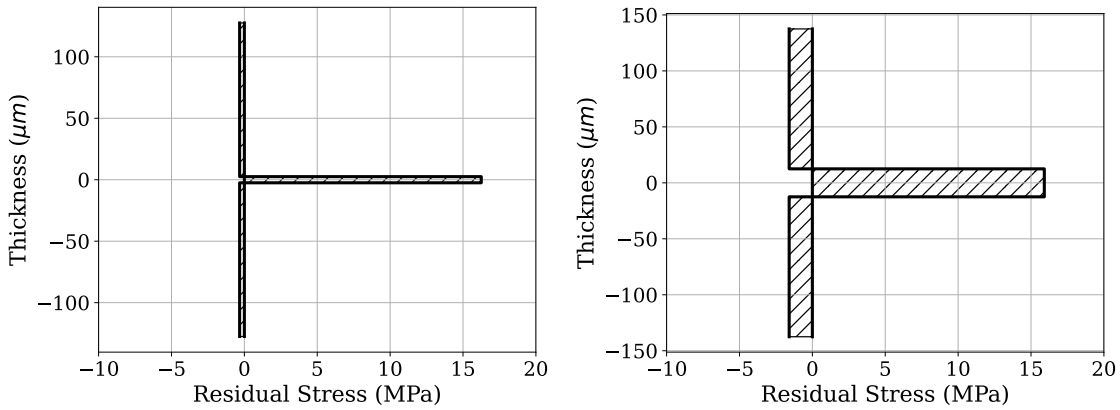


**Fig 4.** Residual stress predictions for the $[0/PEI/0]$ laminate. (Left) 5 $\mu$m PEI thickness, (Right) 25 $\mu$m PEI thickness.

The goal is to reduce the PEI thickness in order to maintain a high fiber-volume fraction in the entire laminate. The residual stress analysis shows that reducing the thickness from 25 to 5 µm led to a negligible increase in residual stress. A $[\mathrm{PEI}/0/\mathrm{PEI}]_{2s}$ stacking sequence represents an OATMEAL laminate where the PEI enables processing below the melt temperature of the CF/PEEK. Reducing the thickness led to a more significant increase in PEI residual stress from 14.91 to 15.99 MPa (see Figure 5) but doubled the CF/PEEK compressive residual stress. It is possible that the higher compressive residual stress with the thicker resin rich layers influences the performance, such as observed in the SBS testing and by Arquier et al [7]. Unfortunately CLT cannot be used to determine the interlaminar shear stress through the thickness (relevant to the SBS results) [9], but it is reasonable to expect these residual stresses to reduce performance. It is of interest to investigate interlaminar stresses with a more advanced model. Lastly, a $[0/\mathrm{PEI}/90/\mathrm{PEI}/0]$ laminate (see Figure 6) shows similar behavior where the compressive residual stresses reduced from -7.04 to -4.34 MPa in the 0° lamina while in the 90° the residual stress increased from 6.29 to 6.70 MPa. The 90° is in tension due to having a larger CTE than the 0° lamina. The predicted PEI residual stress is 17.91 and 18.20 MPa for the 5 and 25 µm thickness, respectively.

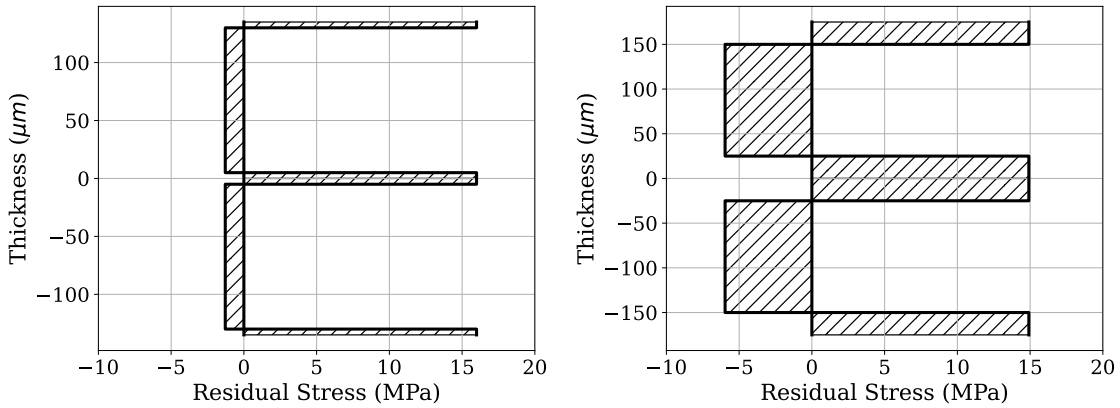


**Fig 5.** Residual stress predictions for the $[PEI/0/PEI]_{2s}$ laminate. (Left) 5 $\mu$m PEI thickness, (Right) 25 $\mu$m PEI thickness.

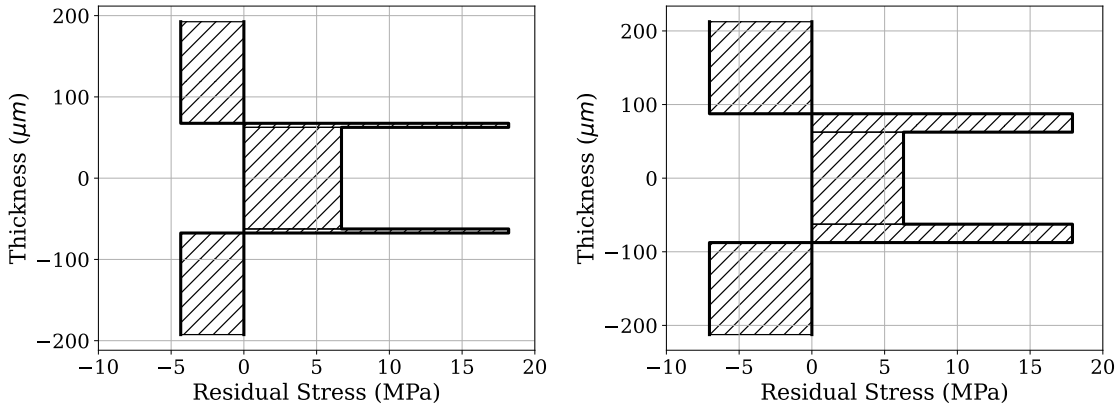


**Fig 6.** Residual stress predictions for the $[0/PEI/90/PEI/0]$: laminate. (Left) 5 $\mu$m PEI thickness, (Right) 25 $\mu$m PEI thickness.

## 5. CONCLUSIONS

Understanding and harnessing the nuances of fusion bonding in thermoplastic composites can be highly beneficial for meeting the high production rates required by the aerospace and automotive industries. In this study, the fact that amorphous polymers can self-heal above their glass transition temperature is used to develop a composite material that can be bonded below the melt temperature of semi-crystalline polymers – resulting in a cooling rate independent material. Thin amorphous PEI films (ranging from potentially 5 to 20 μm-thick) are healed to semi-crystalline LM-PAEK carbon fiber prepreg and then slow-cooled to maximize crystallinity development. Next, the PEI surfaces are healed together, both below and above the melt temperature of LM-PAEK to form a full plate and then fast-cooled. Our findings demonstrate that high SBS, exceeding 80 MPa, can be achieved by processing below the melt temperature of LM-PAEK, while leveraging the self-healing property of the amorphous PEI. However, when healing above the melt temperature of LM-PAEK, the SBS decreases by approximately 15%, influenced by the PEI thickness. This establishes an optimizable relationship between the PEI thickness required to promote fusion bonding (ensuring intimate contact and interdiffusion) and maximizing the overall performance. Investigation into how the PEI thickness influences the residual stress development during manufacturing is considered using CLT. Due to a mismatch in CTEs, the PEI layers are stressed in tension (~16 MPa) whereas 0° CF/PEEK are compressed (~6 MPa) for a $[\mathrm{PEI}/0/\mathrm{PEI}]_{2s}$ laminate. It is observed that reducing the PEI thickness leads to a residual stress increase in the PEI and a reduction in the CF/PEEK; this effect is more pronounced in laminates with PEI at every interface. That being said, minimizing the PEI thickness is important to for maintaining the fiber volume fraction of the composite. While the impact of these residual stresses should be considered, the potential of a cooling-rate independent thermoplastic composite (OATMEAL) with thin amorphous interfaces is demonstrated.

## 6. ACKNOLEDGEMENTS

The authors are grateful for the support provided by NASA NSTGRO grant #80NSSC22K1203.

# 7. REFERENCES


[1] C. Ageorges, L. Ye, and M. Hou, "Advances in fusion bonding techniques for joining thermoplastic matrix composites: a review." [Online]. Available: www.elsevier.com/locate/compositesa

[2] F. Yang and R. Pitchumani, "Healing of thermoplastic polymers at an interface under nonisothermal conditions," *Macromolecules*, vol. 35, no. 8, pp. 3213–3224, Apr. 2002, doi: 10.1021/ma010858o.

[3] Y. M. Boiko, G. Ârald, G. Ârin, V. A. Marikhin, and R. E. Prud'homme, "Healing of interfaces of amorphous and semi-crystalline poly(ethylene terephthalate) in the vicinity of the glass transition temperature." [Online]. Available: www.elsevier.com/locate/polymer

[4] A. J. Smiley, A. Halbritter, F. N. Cogswell, and P. J. Meakin, "Dual polymer bonding of thermoplastic composite structures," *Polym Eng Sci*, vol. 31, no. 7, pp. 526–532, 1991, doi: 10.1002/pen.760310709.

[5] P. J. Meakin, F. N. Cogswell, A. J. Halbritter, A. J. Smiley, and P. A. Staniland, "Thermoplastic interlayer bonding of aromatic polymer composites-methods for using semi-crystallized polymers."

[6] O. Baho, G. Ausias, Y. Grohens, M. Barile, L. Lecce, and J. Férec, "Automated fibre placement process for a new hybrid material: A numerical tool for predicting an efficient heating law," *Compos Part A Appl Sci Manuf*, vol. 144, May 2021, doi: 10.1016/j.compositesa.2021.106360.

[7] R. Arquier, H. Sabatier, I. Iliopoulos, G. Régnier, and G. Miquelard-Garnier, "Role of the inter-ply microstructure in the consolidation quality of high-performance thermoplastic composites," *Polym Compos*, vol. 45, no. 2, pp. 1218–1227, Jan. 2024, doi: 10.1002/pc.27847.

[8] S. V. . Hoa, *Principles of the manufacturing of composite materials*. DEStech Publications, 2009.

[9] Bednarcyk, Brett A., Jacob Aboudi, and Phillip W. Yarrington. *Determination of the Shear Stress Distribution in a Laminate from the Applied Shear Resultant--A Simplified Shear Solution*. No. E-16226, 2007

[10] N. Heathman, P. Koirala, T. Yap, A. Emami, and M. Tehrani, "In situ consolidation of carbon fiber PAEK via laser-assisted automated fiber placement," *Compos B Eng*, vol. 249, no. October 2022, p. 110405, 2023, doi: 10.1016/j.compositesb.2022.110405.